LAMB WAVE BASED MONITORING OF PLATE-STIFFENER DEBODING USING A CIRCULAR ARRAY OF PIEZOELECTRIC SENSORS

V. T. Rathod and D. Roy Mahapatra[1]
Department of Aerospace Engineering, Indian Institute of Science, Bangalore 560012
[1]Email: droymahapatra@aero.iisc.ernet.in

Abstract- In this paper we propose an efficient way of localization and parametric identification of metallic plate-stiffener debonding. A concept and experimental results based on a circular array of Piezoelectric Wafer Active Sensors (PWASs) is presented. Implementation of this circular array of PWASs combines the Lamb wave technique and symmetry breaking in the signal pattern to monitor the growth of a debonding of a stiffener on a metallic plate. Wavelet time-frequency maps of the sensor signals are employed and a damage index is plotted against the damage parameters for frequency sweep of the excitation signal (a windowed sine signal). Wavelet coefficient in time gives an insight regarding the effect of debonding growth on the Lamb wave transmission in time-frequency scale. We present here a method to eliminate the time scale effect which helps in identifying easily the signature of damage in the measured signals including the reflection from the boundary of the plate. The proposed method becomes useful in determining the approximate location of the damage with respect to the location of three neighboring sensors in the circular array. A cumulative damage index is computed for varying damage sizes and the results appear promising.

Index terms*: Circular array, piezoelectric, wavelet, damage index, lamb wave, plate, debonding.*

I. INTRODUCTION

Lamb waves can travel relatively long distances with little amplitude loss in isotropic plates and hence offer large-area coverage. Details of the methods to launch Lamb wave and type of wave modes in plates can be found in standard text [1]. Characteristics of Lamb wave propagation in metallic and composite plates with integrated piezoelectric transducers have been studied extensively in literature (see e.g., references [1-3] and further references therein). In this paper we consider Piezoelectric Wafer Active Sensors (PWASs), which has the capability to generate and

receive ultrasonic Lamb waves for structural health monitoring [4]. As compared to the conventional NDE probes, PWASs are inexpensive, non-intrusive, unobtrusive, and minimally invasive device that can be surface mounted on existing structures or inserted between the layers of lap joints or inside composite laminates. Giurgiutiu [5] developed embedded PWAS to perform in-situ nondestructive evaluation. Rajagopalan et al [6] has studied the concept of PZT sensor/actuator network in large plate structure for identification of crack location and sensitivity of the edge reflection. Apart form the development of PWAS network, development of damage detection and localization algorithm in related context has recently gained much interest. Zhao et al [7] developed a reconstruction algorithm for inspection of defects using arrival time and distance information from circular sensor/actuator network.

Given this background research, there is a significant advantage of a sensor/actuator network, which can be designed such that it occupies less area on a structure but still monitors large area of that structure. Guided ultrasonic waves have been employed over the last several decades for identifying crack location, mainly using the information regarding wave arrival time[8], changes in wave attenuations using wavelets [8,9], time-frequency analysis [10] and wave reflections [11,12]. Several literatures on the quantification of damage using ultrasonic wave based Structural Health Monitoring, including those using wavelet analysis, can be found in literature. Deng and Wang [13] applied discrete wavelet transform to locate a crack along the length of a beam. Quek et al [14] used wavelet analysis for crack identification in beams under both simply supported and fixed–fixed boundary conditions. Douka et al [15, 16] estimated the depth of a crack and defined an intensity factor to relate the wavelet coefficients to the depth of the crack. Nag et al. [17] and Kumar et al. [18] reported a correlation between a frequency domain Damage Force Indicator (DFI) and mode I/II cracks using Lamb wave technique. Keilers and Chang [19], Ihn and Chang [20, 21] and Yang and Chang [22, 23] used piezoelectric transducers for delamination identification in composite plates. Wavelet based damage index analysis was done with the help of piezoelectric transducers on a damaged plate with different crack orientations [24]. A wave-based damage index was formulated for the analysis of the filtered response of damaged beams [25]. Gangadharan et al [26] used wavelet transform and Hilbert–Huang transform to quantify the damage parameters like damage size and material degradation factors. Within the framework of integrated SHM, damages like delamination or debonding, bolted joint failures etc., are challenging and very little has been reported in published literature in these

topics. Damage such as delamination gets initiated and it grows with the applied load particularly in metal structures. Here, the delamination is referred to debonding of stiffener on a plate. In such structures the strength continuously degrades and finally results in failure of the structure. In this paper we report a concept based on a circular array of PWAS which incorporates ultrasonic Lamb wave technique and a symmetry breaking pattern of sensor signals for identification of the location of the damage (delamination) and estimation of damage parameters in terms of signal energy using wavelet transform.

II. CIRCULAR ARRAY OF PIEZOELECTRIC WAFER ACTIVE SENSORS

An array of PWAS arranged in a circular arrangement with radius of 50 mm on a plate was made for laboratory experiment (see figure 1). A PWAS placed at the center of the circular array was used as actuator (A). Another PWAS S4 was placed at the boundary of the plate (see figure 1) for sensing wave packets transmitted through the stiffener. The aluminium plate has dimensions of 600 x 400 mm with thickness of 1 mm. The actuator A was used to excite the ultrasonic Lamb wave and three of the sensors in the circular array S1, S2, S3 and sensor S4 were used to monitor delamination growth. Both the actuation and the sensor signal acquisition were performed using a portable NI PCIe-6259 multifunctional DAQ system and a computer running Labview program. A Labview code with matlab script was created for this purpose, which launches a tone-burst signal with known frequency content and amplitude. To remove the unnecessary noises in the signal, a band-pass filter is used.

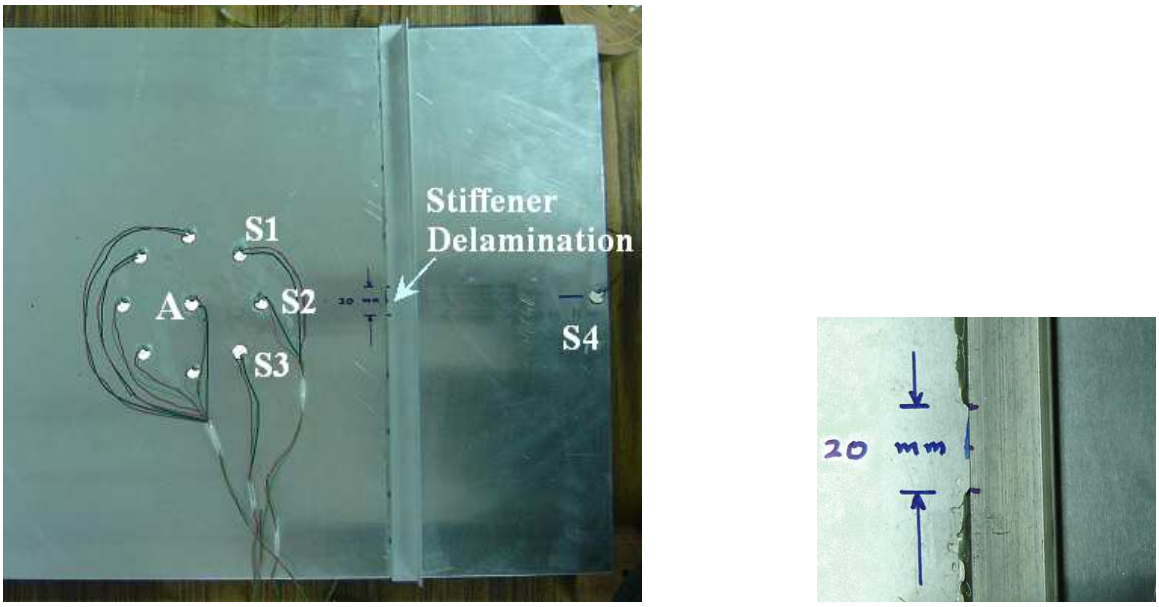

(a) (b)

Figure 1. Experimental setup (a) location of circular array of PWAS with actuator A at center of array and sensors S1, S2 and S3 on the circumference. Sensor S4 is located at the edge of the plate and a stiffener with delamination at center of plate. (b) Enlarged view of damage location.

a. Lamb Wave Transmission and Reflection Paths

The main concept proposed using a circular array of PWAS in the present work is that the identification of damage location can be carried out by identifying and differentiating the arrival time of the reflected wave from the damage using three or more neighboring PWAS in the circular array and by comparing the symmetry breaking pattern. Ultimately, it does not require all the sensor signals to quickly locate the angular orientation of the damage. A schematic diagram of the plate with the location of PWAS array is shown in figure 2. In the present experiments, damage in the form of delamination is created in the plate at one-fourth distance from the shorter edge of the plate and at one-half distance from the longer edge (see figure 1). The damage, the actuator A and the sensor S2 of the circular array lie on a straight line as shown in figure 2. This alignment could be sometime little deviated depending on the number of sensors used in the array. However, the present case constitutes an example configuration, which would be generic enough due to circular symmetry of the sensor array. However, two major uncertainties may be caused, one is due to non-identical bonding of the sensors to the plate and other is if the sensor

array is course and a damage does not lies exactly on the radial line A-S1-Damage. Such practical issues can be addressed later. In the present case, the two sensors S1 and S3 of the circular array are equidistant from the center line A-S2-Damage. The shortest path of the reflected waves from the damage and the boundary of the plate for circular array sensors are shown. For all of these sensors, the wave path-length for reflection from the damage is smaller than the path-length of reflection from the nearest boundary of the plate. This eliminates the chance of the reflected waves from damage and from the boundary of the plate getting mixed for a suitable chosen time window of signal measurement.

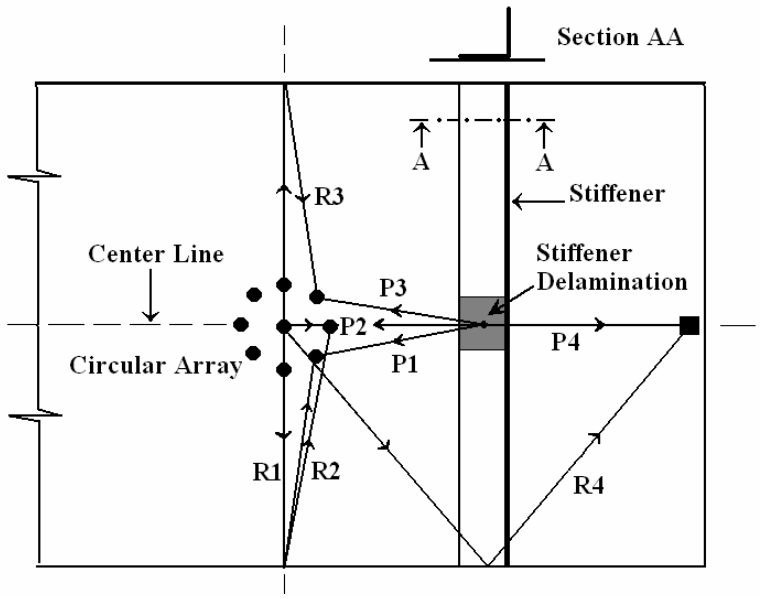

Figure 2. Schematic diagram of a plate with circular array of PWASs (corresponding to the setup in figure 1) showing different wave transmission and reflection paths.

b. Signal Sensitivity of Sensors in the Circular Array

Since the plate is symmetric about the straight line passing through the actuator A, the sensor S2 and the damage, therefore the signals obtained from S1 and S3 are expected to be almost identical. The measured signals are shown in figure 3(a). The two reflected peaks correspond to S0 and A0 modes followed by peaks due to reflections from boundaries, all of which match closely in the signals from S1 and S3. This is according the abovementioned expectation. When there is a damage, which maintains the symmetry about the centerline, the two path lengths for

S1 and S2 corresponding to the first reflected peaks of A0 and S0 modes of lamb wave must match closely, whereas the peaks reflected from the damage and reaching S2 compared to S1 or S3 would differ significantly due to path lengths and asymmetry (see figure 3(b)). Reflected peaks in S1, S3 corresponding to A0 and S0 modes match because the sensors are located at equal distances from the actuator A as shown in figure 2. However if bonding produces significant variation in the stress transfer in the sensor wafers, then there will be differences even in the S1 and S3 signals. Such variations should be avoided by prior calibration.

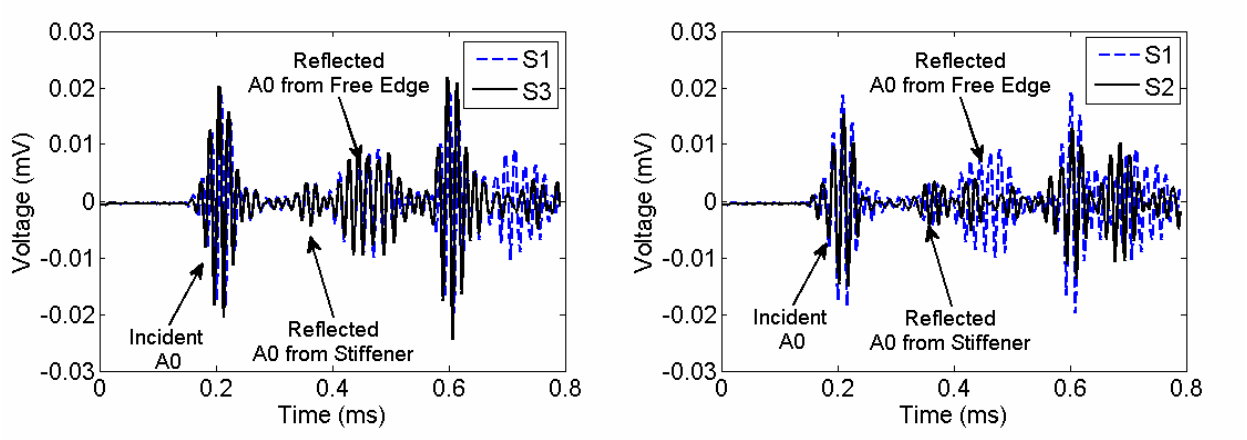

Figure 3. Superimposed sensor signals for 60 kHz modulated sine pulse (a) Signals from S1 and S3 are compared (b) Signals from S1 and S2 are compared. Incident peaks are those due to arrival of the wave from the actuator A.

Presence of any symmetry-breaking damage details about the center line (A-S2-Damage) would shift the reflected wave and also affect their amplitudes and shapes. In such a case, when signals from S1 and S3 are compared, there is a shift observed in the reflected signal due to reflection from the damage. As shown in figure 2, the reflected wave follows the path P1 and P3 for sensors S1 and S3, respectively, which are symmetric. The location of these shifted peaks on the time axis give the arrival time information based on which approximate location of damage can be determined. For an unknown damage location, this would involve a sequence of comparisons using each three neighboring sensors on the array. The presence and severity of damage are determined by a damage index, which is computed from the temporal variation of the wavelet coefficient of the sensor signal. The procedure followed to introduce damage in the plate and

study of wavelet coefficients is elaborated next, followed by a discussion on the cumulative damage index.

III. DAMAGED SAMPLE PREPARATIONS

In the present experiment damage in the stiffened plates is considered with the failure of adhesive bonding between the stiffener and the plate. The delamination between the stiffener and the plate is introduced by partially bonding the stiffener to the plate with an adhesive. To find the severity of the damage, damage size is varied and its effect on wavelet coefficients and damage index is studied. The location of damage is shown in figures 1(a), and figure 1(b) shows the enlarged view of the damage being considered for monitoring. Initially, the sensor signals were acquired for healthy plates. These signals serve as reference signals. After introducing the damages for both cases of damage, the signals were acquired for postprocessing. Another two sets of data are acquired for increment of damage sizes. Various different samples with different length of delamination between stiffener and plate are prepared. Figure 1(b) shows 20 mm delamination introduced between stiffener and plate by avoiding the application of epoxy adhesive in that location while preparing the sample. In this way the data is acquired for various damage sizes and these data are post processed to obtain wavelet coefficients and damage index as discussed in next sections.

IV. WAVELET BASED DAMAGE INDEX

For standard PZT wafers bonded on the plate, the ultrasonic Lamb wave amplitude generally decays with one upon square root of propagation distance in the near-field. Wavelet transform also helps in eliminating such problem due to bonded PZT wafer and signal attenuation. Concentration of the signal energy on the time frequency plane is obtained in terms of the amplitude of the wavelet coefficient at individual frequency scales, the frequency range being that of the excitation signal used. In the present work, we have used continuous wavelet transform, where a given signal of finite energy is projected on a continuous family of frequency bands (or similar subspaces of the function space $L_2(R)$ for instance on every frequency band of the form $[f,2f]$ for all positive frequencies $f>0$). Then, the original signal is reconstructed by a

suitable integration over all the resulting frequency components. The frequency bands or subspaces are the scaled versions of a subspace at scale one. This subspace in turn is generated, in most situations, by the shifts of a generating function $\psi \in L_2(R)$ called the mother wavelet and this function is given by

$$\psi(t) = 2\mathrm{sinc}(2t) - \mathrm{sinc}(t) = \frac{\sin(2\pi t) - \sin(\pi t)}{\pi t} \tag{1}$$

with the (normalized) sinc function. The subspace of scale a or frequency band [1/a, 2/a] is generated by the functions (sometimes called child wavelets)

$$\psi_{a,b,t} = \frac{1}{\sqrt{a}}\psi\left(\frac{t-b}{a}\right) \tag{2}$$

where a is positive and defines the scale and b is any real number and defines the shift. The pair (a,b) defines a point in the right half plane. The continuous wavelet transform of a signal $f(t)$ is then given by

$$W = \int f(t)\psi^*_{a,b,t}dt \tag{3}$$

where the superscript * denotes complex conjugation. This equation shows how a signal $f(t)$ can be decomposed into a set of basis functions $\psi(a,t)$, called the wavelets. The scale factor a is positive and it defines dilation scale factor and b is any real number which defines the shift. These two are the new dimensions in the wavelet after the wavelet transform. For detailed analysis of the ultrasonic lamb wave signal see ref. [26].

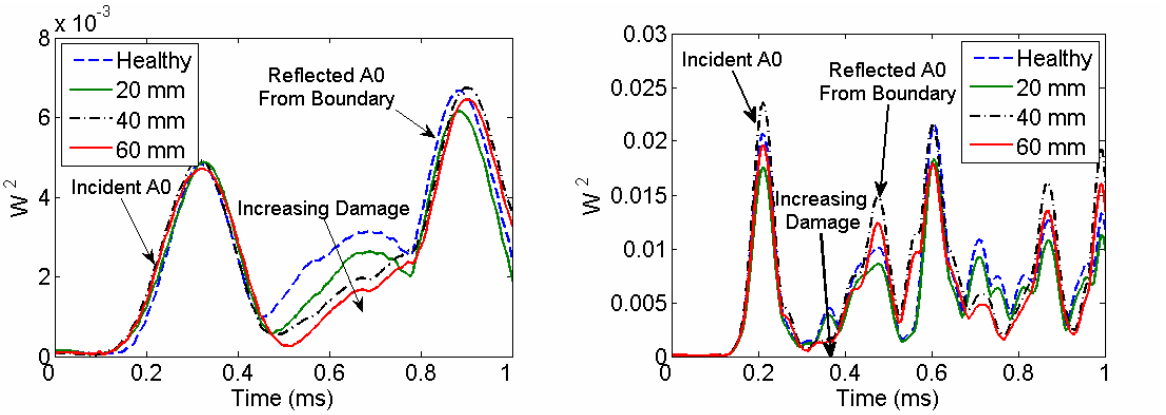

Figure 4. Time history of wavelet coefficient from sensor S2 due to actuation from A (a) for 20 kHz signal frequency (b) for 60 kHz signal frequency.

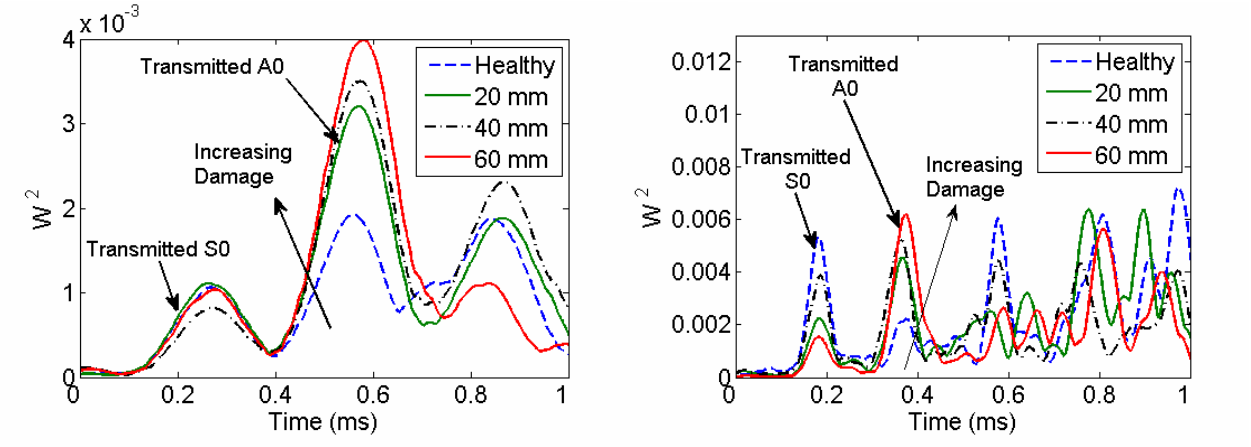

(a) (b)

Figure 5. Time history of wavelet coefficient from sensor S4 due to actuation from A (a) for 20 kHz signal frequency (b) for 60 kHz signal frequency.

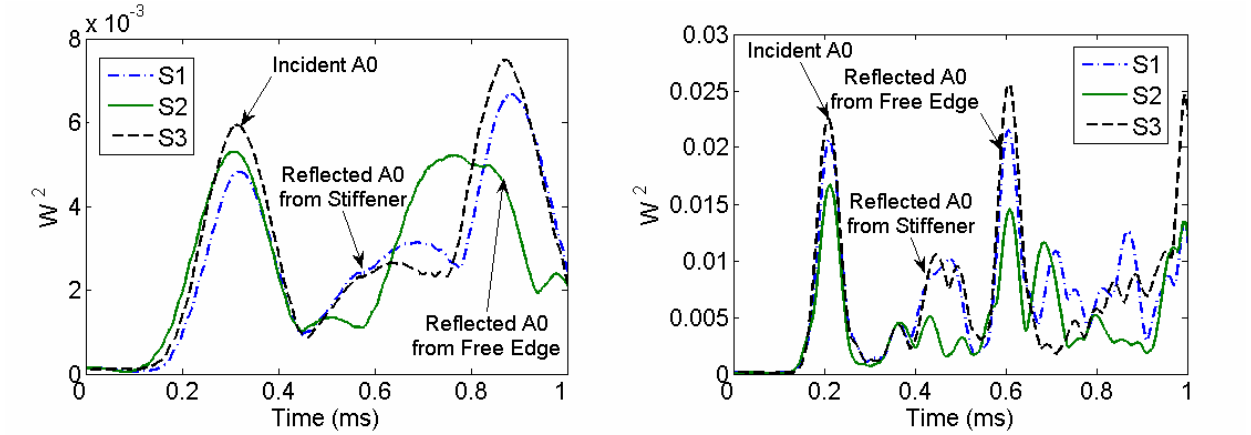

(a) (b)

Figure 6. Comparison among of the wavelet coefficients for signals from various sensors of the circular array (a) for 20 kHz frequency (tone burst incident signal frequency) scale (b) for 60 kHz frequency (tone burst incident signal frequency) scale.

The variations in wavelet coefficient obtained from sensor signal S2 are shown in figure 4 with a single frequency tone burst signals as the actuation signal. In order to monitor the transmitted signal, an actuator A and a sensor S4 are used. The variations of wavelet coefficient obtained from sensor signal S2 is shown in figure 5 with actuation using tone burst signal. As the delamination size increases the contact area between the stiffener and the plate decreases. Lamb

wave energy that is getting transmitted through the bonded interface increases with increasing delamination size. Energy reflected from the stiffener and energy transmitted through the stiffener starts decreasing with delamination size. Thus for sensor S2, the energy reflected by the damage decreases and the wavelet coefficient decreases for the peaks corresponding to the reflected waves (see figure 4). On the other hand for sensor S4, the energy of the signal received by it increases as the delamination size increases (see figure 5). The effect of both types of damages as monitored using the sensors of the circular array can be seen clearly in figures 4 and 5.

Variations in the time histories of wavelet coefficients for signals from the three neighboring sensors of the circular array are also compared in figure 6 for various different frequencies of excitation (tone burst incident signal frequency). It can be seen that the wavelet coefficients match closely for sensors S1 and S3 since their locations are symmetric about the center line of the plate and the damage growth is also symmetric about the path A-S1-Damage. The first peak corresponds to the first incident wave of A0 mode and its location on time scale is same due to equal distance of all sensors from actuator A. The peaks of reflected waves from the nearest boundary of the plate corresponding to S0 and A0 wave modes are also shown in figure 6. The reflected waves from other boundaries also follow these first set of reflected packets since the time window for each wave mode in this case is small due to higher frequency. Since the damage information is present in the signal within the first reflection from the nearest edge, subsequent reflected peaks are not considered in the analysis. The detailed procedure for estimating this and wavelet based damage index is explained in the next section.

a. Time scale elimination

In order to make the interpretation easy and fast, the temporal variation of wavelet coefficient within a particular time window is considered. This time window is set according to the A0 wave packet location on the time axis as received by the sensor. It can be seen in figure 2 that the paths of wave reflected from damage and arriving to the circular array sensors are P1, P2 and P3 for sensors S1, S2 and S3, respectively. Paths P1 and P3 are identical for the damage located on the center line A-S1-Damage. The shortest path of the reflected signal from boundary traces the path

R1 for sensor S1 and S3 and path R2 for S2. The time required for A0 wave mode to travel any distance L can be computed as

$$t = \frac{L}{C_g} \tag{4}$$

where C_g is the group speed of A0 mode found experimentally, and for 60 kHz frequency, it is 1750 m/s. The time required for the excited wave to reach a sensor from actuator A through the shortest path is taken as the incident time t_e and is same for all sensors of the circular array. Based on the shortest path, the time t_r taken for the reflected wave from the damage to reach a sensor is computed. To ensure that the waves reflected from boundary do not get mixed up with the waves reflected from damage and arrive at the sensors, the time t_r should be kept sufficiently larger than time t_e. In a practical problem, this can be achieved by choosing suitable diameter of the circular array and the frequency of the excitation signal. The range of time $[t_e, t_r]$ is considered for analysis in the next section.

b. Normalized Wavelet Coefficient

Any change in the wavelet coefficients with respect to the healthy/updated monitoring stage of the plate is due to the presence of damage, lamb wave mode conversion due to structural boundary reflections or due to variation in ambient noise. We first normalize the wavelet coefficient, which makes it easier to determine the possible location of the damage. If the hidden information due to damage is separated from other information by proper means, localization of damage feature in the processed signal is possible. Once the damage is detected in the structure, it is necessary to determine the location of that damage. This can be done efficiently using time history of the normalized wavelet coefficient. We define the normalized wavelet coefficient as

$$W_N = \left| \frac{W_H^2 - W_D^2}{W_H^2} \right| \tag{5}$$

where W_H and W_D are the wavelet coefficients computed from signals obtained for healthy plate and damaged plate, respectively. The normalized wavelet coefficient is of interest within a time range of $t = t_e$ and $t = t_r$ as shown in figure 7. The time of occurrence of any significant

change in the time derivative of the normalized signal (equation (5)) noticed at the earliest is noted as t_w. This time stamp is obtained corresponding to the three sensors of the circular array. Figure 8 shows the normalized wavelet coefficient as defined in equstion (5) for both types of damages being considered from which the time t_w is obtained that lies in the time range indicated by the two lines. The wave arrival time is then given by

$$t_a = t_w - t_e \tag{6}$$

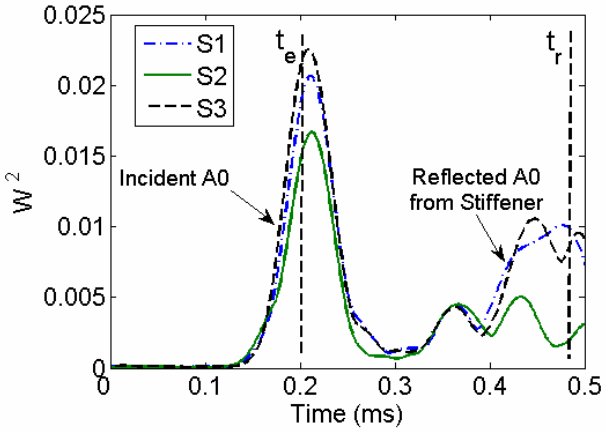

Figure 7. Wavelet coefficient variation at 60 kHz frequency computed from signals of sensors S1, S2 and S3 for delamination of 20 mm.

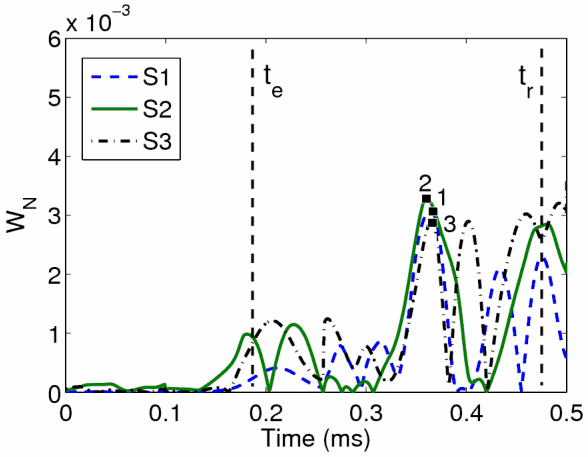

Figure 8. Normalized wavelet coefficient variations at 60 kHz frequency computed from signals of sensors S1, S2 and S3 for delamination of 20 mm.

The arrival time of individual packet with different wave speeds depends on the path-length of the reflected wave from damage for a particular mode of Lamb wave (here the A0 mode). With

the help of group speed of the A0 mode determined experimentally, the distance between the damage and the sensor can be computed using equation (4). The actual distances of the sensors S1, S2, S3 from the damage are 0.220 m, 0.200 m and 0.220 m, respectively. These values can be compared with the experimental values according to table 1 for delamination size of 20 mm. It can be seen that the experimental values are quite accurate.

Table I. Distance calculation using 60 kHz signal for Delamination of 20 mm.

Sensor	t_0 (ms)	t_w (ms)	t_a (ms)	L_p (m)	Error(%)
1	0.214	0.348	0.134	0.2345	6.59
2	0.214	0.322	0.108	0.189	5.5
3	0.214	0.345	0.131	0.2292	4.20

Using the path length for the 3 sensors S1, S2, S3 and geometric relations, the location of the damage can be computed. Thus with the circular array of sensors, both the parametric sensitivity and damage location is possible to identify with good accuracy using the proposed method. With proper algorithm and use of all of the sensors in the circular array in sequence of three neighboring sensors, a whole plate can be monitored for damage. A variation in the time histories of the wavelet coefficients are used to evaluate a damage index, which represents the parametric sensitivity of the damage as discussed next.

V. WAVELET BASED DAMAGE INDEX

In order to locate the damage, it is necessary to detect the presence of damage in the structure. On the other hand, a damage index can be one which quantifies the extent or severity of damage(s). One of such damage index is obtained by integrating the particular region of energy concentration in the time-frequency plane. In the present study, we introduce a damage index (J) in terms of cumulative energy of the signal $f(t) \leftrightarrow \psi(\omega_n, t)$ as

$$J = \frac{1}{\Delta t} \sum_{n_1}^{n_2} \int_0^{\Delta t} |W_N(t)|^2 dt \qquad (7)$$

where Δt is the time window of the region of reflected A0 wave packet being considered in the time-frequency plane. The range $[\omega_{n1}, \omega_{n2}]$ describes the frequency band used in a band-pass FIR filter and applied to the sensor signals. Corresponding contributions from the sampling frequencies are summed up in equation (3). Figure 9 shows the variation in damage index J for various different frequencies with increase in delamination size obtained using transmitted A0 signals of sensors S1, S2, S3 and S4. The frequencies on the x-axis in these figures are actually the frequency of the tone-burst signal used. The incident signal has this frequency as the primary frequency and a narrow frequency band surrounding it which carries the details of launched wave packet shape and its interaction with damage.

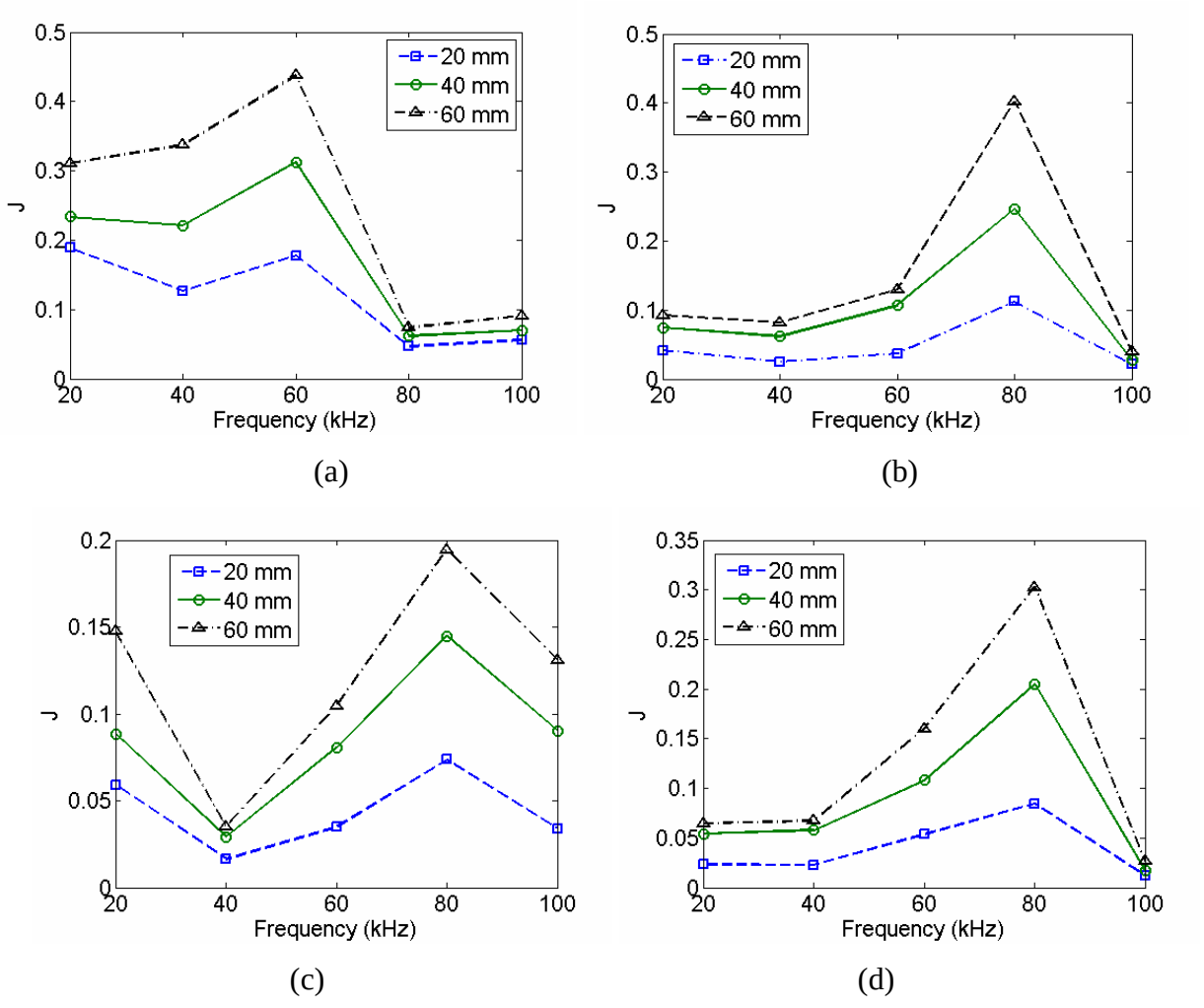

Figure 9. Damage index J for different frequencies obtained using transmitted A0 signals (a) from sensor S4 (b) from sensor S1 (c) from sensor S2 (d) from sensor S3.

Damage index J increases monotonically with increase in the damage size for almost all frequencies of excitation considered in this work. The damage index is sensitive to frequency, for example, for 80 kHz signal, the sensitivity is high for sensors S1, S2 and S3. The damage index in smallest at 80 kHz and high at 60 kHz for sensor S4. The variation in damage index is well distinguished for sensor S4 and the other sensors of the circular array. Thus parametric sensitivity of the damage can be characterized without the use of transmitted signal from sensor S4. Thus the choice of circular sensor array is a compact one (i.e. without the sensors scattered at many places). Also, the present results demonstrate for the first time the use of wavelet signal in conjunction with the circular array concept to monitor the damage with stiffener debonding as a complex and practical example.

VI. CONCLUSIONS

A concept and experimental results based on circular array of PWASs are reported. Growth of delamination was monitored using Lamb wave technique and symmetry breaking pattern in the signal acquired by the circular array of PWASs. Parametric sensitivity for damages in a plate such as delamination growth is obtained in terms of damage index. One of the PWAS located at the center of the circular array was used as an actuator and parametric sensitivity due to damage was studied using signals from sensors of circular array with symmetric arrangement and the approach is found to be successful. The time scale elimination technique can be used in algorithms for fast identification of arrival time. Normalized wavelet coefficient gives the time of arrival information of the reflected wave from the damage. This arrival time is used to calculate the path lengths for sensors and finally the location of damage. The error in the estimated location of delamination is within 6.59%. The location is identified using a circular array of PWAS sensors with reference to usual one pair of sensor-actuator approach. Thus a circular array of PWAS can independently work without requirement of other sensors or actuators on structure and with much smaller physical coverage area. The monotonic increase in damage index for different frequencies was obtained by analysis of the reflected A0 wave. This gives a way for efficient parametric estimation of delamination with time. Damages located on other parts of the

plate can be monitored with the use of other sensors of the circular array and the whole sequence can be automated using a suitable algorithm.

REFERENCES

[1] J.L.Rose, "Ultrasonic waves in solid media. Cambridge", U.K. Cambridge University Press, 1999, pp. 101-113.

[2] D.Roy Mahapatra, A.Singhal, and S. Gopalakrishnan, "Lamb wave characteristics of thickness-graded piezoelectric IDT", Ultrasonics, Vol, 43, No. 9, 2005, pp. 736-746.

[3] D.Roy Mahapatra, A.Singhal, S.Gopalakrishnan, "Numerical analysis of piezoelectric composite IDT for lamb wave generation", IEEE Trans on Ultrasonics, Ferroelectrics and Frequency Control, Vol. 50, No. 10, 2005, pp. 1851-1860.

[4] V.Giurgiutiu, "Multifunctional vehicle structural health monitoring opportunities with piezoelectric wafer active sensors", 44th AIAA/ASME/ASCE/AHS Structures, Structural Dynamics and Materials Conference, 7-10 April 2003, Norfolk, Virginia.

[5] V.Giurgiutiu, "Embedded NDE with piezoelectric wafer-active sensors in aerospace applications", J. Mater., Online special issue on Nondestructive Evaluation, 2003.

[6] J.Rajagopalan, K.Balasubramaniam, C.V.Krishnamurthy, "A single transmitter multi-receiver (STMR) PZT array for guided ultrasonic wave based structural health monitoring of large isotropic plate structures", Smart Mater. Struct., Vol. 15, 2006, pp. 1190–1196.

[7] X.Zhao, H.Gao, G.Zhang, B.Ayhan, F.Yan, C.Kwan, J.L.Rose, "Active health monitoring of an aircraft wing with embedded piezoelectric sensor/actuator network: I. Defect detection, localization and growth monitoring", Smart Mater. Struct., Vol. 16, 2007, pp.1208–1217.

[8] S.S.Kessler, "Piezoelectric-based in-situ damage detection of composite materials for structural health monitoring systems", MIT, Massachusetts. Ph.D. Dissertation, 2002.

[9] H.Sohn, G.Park, J.R.Wait, N.P.Limback, C.R.Farrar, "Wavelet-based signal processing for detecting delamination in composite plates", Smart Mater. Struct., Vol. 13, 2004, pp. 153–160.

[10] M.Lin, X.Qing, A.Kumar, S.Beard, "Smart layer and smart suitcase for structural health monitoring applications", Proceedings of SPIE, Vol. 4332, 2001, pp. 98-106.

[11] V.Giurgiutiu, A.Zagrai, J.J.Bao, "Piezoelectric wafer embedded active sensors for aging aircraft", Struct. Health Monitor., Vol. 1, 2002, pp. 41-61.

[12] M.Lemistre, D.Balageas, “Structural Health Monitoring System based on Diffracted Lamb Wave Analysis by Multiresolution Processing”, Smart Mater. Struct. Vol. 10, 2001, pp. 504-511.

[13] X.Deng, Q.Wang, “Crack detection using spatial measurements and wavelets”, Int. J. Fract. Vol. 91, 1998, pp. 23–28.

[14] S.Quek, Q.Wang, L.Zhang, K.Ang, “Sensitivity analysis of crack detection in beams by wavelet techniques”, Int. J. Mech. Sci. Vol. 43, 2001, pp. 2899–2910.

[15] E.Douka, S.Loutridis, A.Trochidis, “Crack identification in plates using wavelet analysis”, J. Sound Vibrat., Vol. 270, 2004, pp. 279–295.

[16] J.W.Xiang, X.F.Chen, B.Li, Y.M.He, Z.J.He, “Identification of a crack in a beam based on the finite element method of a B-spline wavelet on the interval”, J. Sound Vibrat., Vol. 296, 2006, pp. 1046–1052.

[17] A. Nag, D.Roy Mahapatra, S.Gopalakrishnan, T.S.Sankar, “A spectral finite element with embedded delamination for modeling of wave scattering in composite beams”, Compos. Sci. Technol. Vol. 63, 2003, pp. 2187–2200.

[18] D.S. Kumar, D. Roy Mahapatra, S.Gopalakrishnan, “A spectral Fnite element for wave propagation and structural diagnostic analysis of composite beam with transverse crack”, Finite Elem. Anal. Des. Vol. 40, 2004, pp. 1729-1751.

[19] C.H.Keilers, and F.K.Chang, “Identifying delamination in composite beams using built-in piezoelectrics”, J. Intell. Mater. Syst. Struct., Vol. 6, 1995, pp. 649–672.

[20] J.B.Ihn, F.K.Chang, “Detection and monitoring of hidden fatigue crack growth using a built-in piezoelectric sensor/actuator network I. Diagnostics”, Smart Mater. Struct., Vol. 13, 2004, pp. 609–620.

[21] J.B.Ihn, F.K.Chang, “Detction and monitoring of hidden fatigue crack growth using a built-in piezoelectric sensor/actuator network: II. Validation using riveted joints and repair patches”, Smart Mater. Struct., Vol. 13, 2004, pp. 621–630.

[22] J.Yang, F.K.Chang, “Detection of bolt loosening in C–C composite thermal protection panels: I. Diagnostic principle”, Smart Mater. Struct., Vol. 15, 2006, pp. 581–590.

[23] J.Yang, F.K.Chang, “Detection of bolt loosening in C–C composite thermal protection panels: II. Experimental verification”, Smart Mater. Struct., Vol. 15, 2006, pp. 591–599.

[24] M.Panchal, “Lamb wave based structural health monitoring of damaged plate with piezoelectric transducers and development of wavelet based damage index”, Dept. of Aerospace Engg, I.I.Sc. Bangalore, M.E. Thesis, 2008.

[25] S.Gopalakrishnan, N.Apetre, M.Ruzzene, “A wave-based damage index for the analysis of the filtered response of damaged beams”, J. Mech. Materi. Struct., Vol. 3, No. 9, 2008, pp.1605-1623.

[26] R.Gangadharan, D.Roy Mahapatra, S.Gopalakrishnan, C.R.L.Murthy, M.R.Bhat, “On the sensitivity of elastic waves due to structural damages: Time–frequency based indexing method”, J. Sound Vibrat., Vol. 320, No. 4, 2009, pp. 915–941.